8578 *Biochemistry* **2009,** *48,* 8578–8584
DOI: 10.1021/bi900872p

BIOCHEMISTRY
including biophysical chemistry & molecular biology
Article

^{19}F NMR Studies of α-Synuclein Conformation and Fibrillation†

Conggang Li,‡ Evan A. Lutz,‡ Kristin M. Slade,‡ Rebecca A. S. Ruf,‡ Gui-Fang Wang,‡ and Gary J. Pielak*,‡,§

‡*Departments of Chemistry and* §*Biochemistry and Biophysics and Lineberger Comprehensive Cancer Center, University of North Carolina at Chapel Hill, Chapel Hill, North Carolina 27599*

Received May 22, 2009; Revised Manuscript Received July 31, 2009

ABSTRACT: Fibrils of the intrinsically disordered protein α-synuclein are hallmarks of Parkinson's disease. The fluorescent dye thioflavin T is often used to characterize fibrillation, but this assay may not provide quantitative information about structure and mechanism. To gain such information, we incorporated the ^{19}F-labeled amino acid, 3-fluorotyrosine, into recombinant human α-synuclein at its endogenous tyrosine residues. Tyrosine 39 is in the positively charged N-terminal region of this 140-residue protein. The other three tyrosines, 125, 133, and 136, are near the C-terminus. ^{19}F nuclear magnetic resonance spectroscopy was used to study several properties of labeled α-synuclein, including its conformation, conformational changes induced by urea, spermine, and sodium dodecyl sulfate (SDS), its interaction with SDS micelles, and the kinetics of fibril formation. The results show that the tyrosines are in disordered regions but that there is some structure near position 39 that is disrupted by urea. SDS binding alters the conformation near position 39, but the C-terminal tyrosines are disordered under all conditions. The NMR data also indicate that SDS−micelle-bound α-synuclein and the free protein exchange on the 10 ms time scale. Studies of fibrillation show the utility of ^{19}F-labeled NMR. The data indicate that fibrillation is not accompanied by the formation of large quantities of low molecular weight intermediates. Although dye binding and ^{19}F NMR data show that 1 mM SDS and 1 mM spermine accelerate aggregation compared to buffer alone, only the NMR data indicate that the species formed in SDS are smaller than those formed in buffer or buffer plus spermine. We conclude that ^{19}F NMR spectroscopy is useful for obtaining residue-level, quantitative information about the structure, binding, and aggregation of α-synuclein.

α-Synuclein is 140 amino acids long with three distinct regions. The N-terminal region is positively charged, the hydrophobic core comprises residues 61−90, and the C-terminal region is negatively charged (*1*). As shown in Figure 1A, the protein has four unevenly distributed tyrosines, one (Y39) near the N-terminus and three (Y125, Y133, and Y136) near the C-terminus.

Monomeric α-synuclein is disordered and forms amyloid-like fibrils (*1*−*9*). These fibrils are major components of Lewy bodies, the hallmark of Parkinson's disease (*10*). The fibrils are linear rods, 5−10 nm in diameter, much like those seen in other amyloid diseases (*3*). The fibrils form insoluble cross-*β*-sheets, and fibril growth in vitro exhibits a sigmoidal time dependence (*11*, *12*). Prior to the growth phase is a lag, the length of which depends on conditions, such as concentration and pH. Following the lag is a period of elongation in which the fibril concentration increases exponentially and then plateaus (*13*). NMR and other techniques have been used to characterize the structure and dynamics of α-synuclein in solution and in fibrils. Nevertheless, the mechanism by which the mainly disordered monomer assembles into stacked *β*-sheet structured fibrils is unclear.

Fibril growth can be monitored with thioflavin T (ThT)[1]. This dye experiences a shift in excitation and emission when bound to *β*-sheets in fibrils (*14*). Although ThT fluorescence is frequently used to assess α-synuclein fibrillation, the specificity and efficiency of ThT binding vary with fibril morphology and structure (*15*−*17*). Small molecules can also affect its fluorescence. Thus, ThT may not provide unambiguous information and cannot provide residue-level information. Fink and co-workers have used a variety of techniques, including Fourier transform infrared resonance, circular dichroism, and light scattering, to characterize α-synuclein fibrillation (*6*, *18*, *19*). These studies suggest the existence of intermediate states prior to fibril formation.

The ^{19}F chemical shift is known for its sensitivity to the environment and hence should be a good reporter of conformational changes during fibrillation (*20*, *21*). Furthermore, adding a few fluorine atoms to a protein has a minimal effect on structure and dynamics (*22*). For instance, Winkler et al. (*23*) incorporated 5-fluorotryptophan into α-synuclein at three positions and found only minor differences in the microenvironment. Here we report selective incorporation of 3-fluorotyrosine (fY) into α-synuclein (Figure 1A) and the use of ^{19}F NMR to characterize the labeled proteins and assess its fibrillation.

MATERIALS AND METHODS

^{19}F-Labeled α-Synuclein. Site-directed mutagenesis was carried out by using the QuickChange system (Stratagene) with the following mutagenic primers: Y125F, 5′CCTGACA-ATGAGGCTTTTGAAATGCCTTCTGAG3′; Y133F, 5′CTT-CTGAGGAAGGGTTTCAAGACTACGAACC3′; and Y136F, 5′GCCTTCTGAGGAAGGGTACCAAGACTTCGAACCT-GAAG CCTAAC3′.

†This work was supported by a NIH Director's Pioneer Award (DP1OD783) to G.J.P. and a Foundation for Aging Research Glaxo-SmithKline Foundation Award to R.A.S.R.

*To whom correspondence should be addressed. Phone: (919) 966-3671. Fax: (919) 843-1580. E-mail: gary_pielak@unc.edu.

[1]Abbreviations: fY, 3-fluorotyrosine; NMR, nuclear magnetic resonance; PAG, polyacrylamide gel; PBS, phosphate-buffered saline; SDS, sodium dodecyl sulfate; ThT, thioflavin T.

 Published on Web 08/05/2009

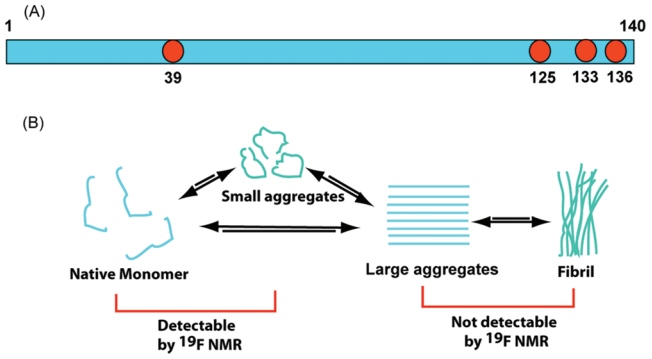

FIGURE 1: Cartoon illustrations showing the location of the tyrosine residues in α-synuclein (A) and the fibrillation process indicating the detectability of species by solution NMR (B).

The incorporation of fY into α-synuclein was achieved by using a slight modification of a previous procedure (*24*). Ampicillin was added to a final concentration of 0.1 g/L to all media, and all water was distilled and deionized. A single colony of *Escherichia coli* strain BL21 DE3 Gold harboring the pT7-7 plasmid was used to inoculate 50 mL of Luria−Bertani media (10 g/L Bacto-Tryptone, 5 g/L Bacto-yeast extract, and 10 g/L NaCl). The culture was shaken overnight at 37 °C. Between 7 and 10 mL of the culture was used to inoculate 100 mL of 2×TY media (16 g/L Bacto-Tryptone, 10 g/L Bacto-yeast extract, 5 g/L NaCl, 1 mM NaOH). The culture was shaken at 37 °C until the optical density at 600 nm of a 1 cm path length sample (OD_{600}) reached 0.8. The cells were harvested by centrifuging at 2600*g* for 10 min. The pellet was resuspended in 1 L of M9 media, which is made by combining 200 mL of M9 salts (64 g/L $Na_2HPO_4 \cdot 7H_2O$, 15 g/L KH_2PO_4, 2.5 g/L NaCl, 5 g/L NH_4Cl, 1 M $MgSO_4$), 2 mL of 1 M $MgSO_4$, 10 mL of 40% (w/v) glucose, and 100 μL of 1 M $CaCl_2$ followed by diluting the mixture to 1 L. Cells were grown to an OD_{600} of 0.4 and then supplemented with 0.5 g of glyphosate, 70 mg of *m*-fluoro-D, L-tyrosine (Sigma-Aldrich), 60 mg of L-tryptophan, and 60 mg of L-phenylalanine. The culture was then grown to an OD_{600} of 0.8. α-Synuclein expression was induced with isopropyl *β*-D-1-thiogalactopyranoside (1 mM final concentration). The culture was incubated overnight with shaking at 37 °C. The protein was purified as previously described (*25*), except that the freeze−thaw step was eliminated. The protein purity was assessed with SDS−polyacrylamide gel (PAG) electrophoresis and mass spectrometry. The typical yield of pure protein is ~15 mg from 1 L of saturated culture.

Mass Spectrometry. Samples were desalted and concentrated with C4 ZipTips (Millipore Corp.). The tip was then washed with water and eluted with 5 μL of a 50:50 (v/v) solution of water and acetonitrile containing 0.1% (v/v) formic acid. Nanoelectrospray mass spectrometry was performed on an Applied Biosystems QSTAR-Pulsar QqTof instrument. The sample, comprising 1 μL of eluant, was loaded into a borosilicate nanospray needle (ES381; Proxeon Corp.). The instrument was calibrated with renin substrate (DRVYIHPFHLVIHN, 1.7589 kDa; Sigma-Aldrich). Spectra were deconvoluted with BioAnalyst software (Applied Biosystems).

Fibrillation. Reactions (600 μL) comprised 200 μM α-synuclein in phosphate-buffered saline (PBS; 2.29 g/L Na_2HPO_4, 0.524 g/L $NaH_2PO_4 \cdot H_2O$, 5.51 g/L NaCl, pH 7.4) containing 1 mM EDTA and 500 μM phenylmethanesulfonyl fluoride. Fibril formation was induced at 37 °C by agitation in a New Brunswick I-26 shaker at 225 rpm. Samples (10 μL) were removed and combined with 100 μL of aqueous 250 μM ThT (Sigma-Aldrich). Fibril growth was assessed from the emission at 482 nm. The fluorescence was measured in 96-well plates by using a Molecular Devices SpectraMAX Gemini EM microplate spectrofluorometer with the excitation wavelength set at 442 nm. The ThT-containing samples were discarded after measurement. Control assays with ThT indicate that fluorinated and nonfluorinated α-synucleins have similar fibrillation rates.

Electrophoretic Analysis of Fibrils. Fibrils were separated from smaller species by centrifugation at 17000*g* for 10 min. Fibrils (pellet) and smaller aggregates (supernatant) were treated with SDS and boiled for 10 min before analysis. Eighteen-lane 18% Tris-HCl Criterion gels (Invitrogen) were electrophoresed for 75 min at 200 V. Coomassie-stained gels were analyzed by using a VersaDoc MP imager (Bio-Rad).

^{19}F NMR. Spectra were acquired on a Varian Inova 600 spectrometer equipped with a ^{19}F-{^1H} *z*-gradient probe. The samples (pH 7.4) contained 10% (v/v) D_2O, 50 mM PBS, 1 mM EDTA, and 500 μM phenylmethanesulfonyl fluoride. Spectra were recorded with a 40 kHz sweep width at 37 °C unless noted otherwise. Each spectrum comprised 32K complex points of 512 or 1024 pulses with a recycling delay of 2 s. Proton decoupling was not applied to all spectra. All other acquisition and processing parameters were kept the same to facilitate sample-to-sample comparisons. Chemical shifts are referenced to trifluoroacetic acid at 0 ppm. For fibrillation studies, the samples were returned to the appropriate reaction after spectroscopy.

RESULTS

Mass Spectrometric Analysis of Labeled and Unlabeled α-Synuclein. fY labeling was characterized by using electrospray ionization mass spectrometry. Figure 2 shows the spectrum of the labeled protein. The smallest species has a mass of 14461 amu, consistent with the calculated value of 14461 Da for the unlabeled protein. The other major species have molecular masses of 14478, 14495, 14515, and 14535 Da, consistent with proteins containing one through four fY residues. The relative peak heights are consistent with random labeling. The origin of the two minor species that appear to contain five and six fluorine atoms is unclear.

^{19}F NMR Resonance Assignments. As expected, we observe four resonances in samples of fY-labeled α-synuclein (Figure 3). ^{19}F assignments were obtained by changing tyrosine residues, one at a time, to phenylalanine. The spectrum of each variant lacks one resonance compared to the fully labeled wild-type protein. The free fY in cell lysates was used as an internal chemical shift standard.

Perturbing the ^{19}F Chemical Shift. Figure 4 shows spectra of fY-labeled α-synuclein in isotopic waters containing 90% H_2O/10% D_2O (v/v) and 100% D_2O. Increasing the amount of D_2O causes all four resonances to shift to higher field by 0.21 ppm. Figure 5 shows spectra of labeled α-synuclein in buffer, 8 M urea, and 200 mM SDS. The chemical shifts of the three C-terminal residues are the same in SDS, urea, and buffer. The fY39 resonance shifts to higher field in urea and SDS. The largest shift change, ~0.35 ppm, is observed in SDS and is accompanied by broadening of the fY39 resonance.

SDS−Micelle Interactions. The spectra in Figure 6 were acquired with 200 μM α-synuclein as a function of SDS concentration. The intensity of the fY39 resonance decreases with increasing SDS concentration. When the SDS concentration

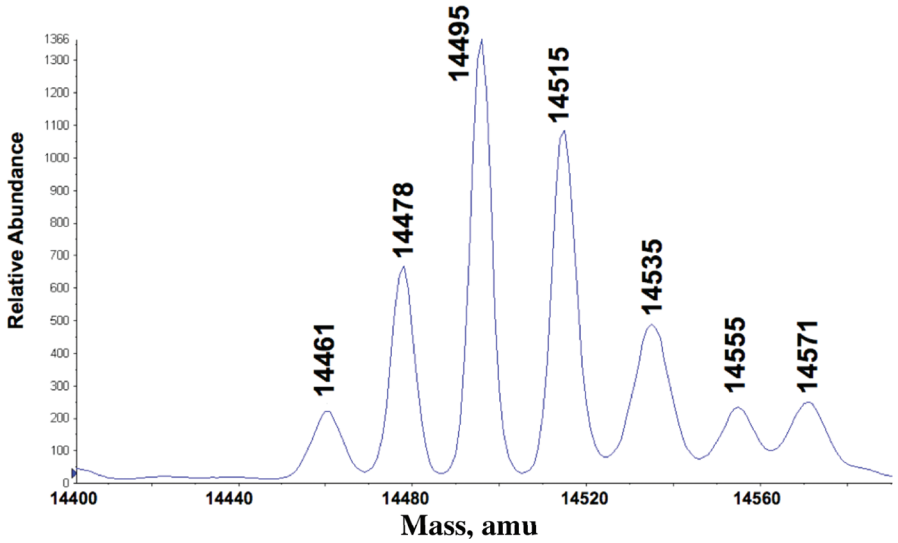

FIGURE 2: Deconvoluted mass spectrum of fY-labeled α-synuclein.

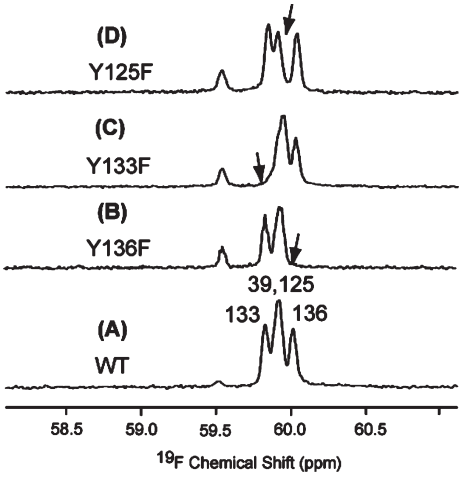

FIGURE 3: ^{19}F NMR spectra and assignments of wild-type α-synuclein (A) and the Y136F (B), Y133F (C), and Y125F (D) variants in cell lysates. The arrows show the position of the resonance that disappears in each variant. The resonance at 59.4 ppm is from free fY.

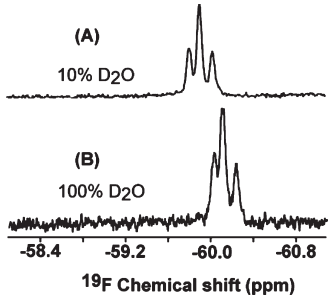

FIGURE 4: ^{19}F NMR spectra of α-synuclein in 10% (v/v) D_2O (A) and 100% D_2O (B).

reaches 12 mM, a new broad resonance appears whose intensity increases with SDS concentration. The temperature dependence was also examined (Figure 7). In 6 mM SDS at 37 °C, the fY39 resonance is too broad to detect. When the temperature is increased to 60 °C, a new resonance appears at −59.7 ppm, and the whole spectrum shifts to lower field. In 18 mM SDS, the new fY39 signal is present at both 37 and 60 °C and sharpens at the higher temperature.

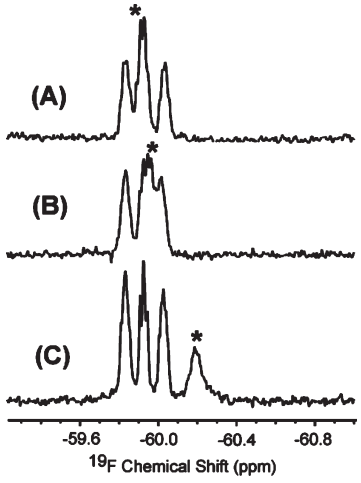

FIGURE 5: ^{19}F NMR spectra of 200 μM α-synuclein in buffer (A), 8 M urea (B), and 200 mM SDS (C). An asterisk indicates the position of the fY39 resonance.

Time Course Experiments. We studied α-synuclein fibrillation under four conditions: buffer alone and buffer plus 1 mM SDS, 5 mM SDS, or 1 mM spermine. Figure 8 shows ^{19}F spectra as a function of incubation time. At zero time, the spectrum in spermine is the same as that in buffer. In SDS, the fY39 resonance from the free form broadens and is undetectable in 5 mM SDS. The resonances decrease in intensity after 2 days, with the fY39 resonance decreasing faster than those of the C-terminal residues. No chemical shift changes or new resonances are observed during fibril formation under any conditions. The signal loss plateaus after 6 days for all of the samples.

Comparing ThT Fluorescence Data to ^{19}F NMR Data. The kinetics of α-synuclein fibrillation were monitored by fluorometry and ^{19}F NMR spectrometry. Figure 8 shows the time dependence of the NMR spectra acquired in buffer, 1 mM spermine, 1 mM SDS, and 5 mM SDS at 37 °C. Figure 9 shows their fluorescence intensities and integrated ^{19}F signals as a function of time. Samples for fluorometry and NMR analysis were removed at the same time. The time course for the NMR data is similar to that for ThT except for the 1 mM SDS sample, where the NMR data suggest less fibril formation.

Figure 10 shows the SDS−PAG analysis of fibrillation. The soluble supernatant samples represent monomer and small aggregates. The pellets represent the high molecular mass fibrils. Most of the α-synuclein is in the pellets from fibrillation experiments conducted in buffer and spermine. In SDS, however, most of the protein is in the soluble fraction.

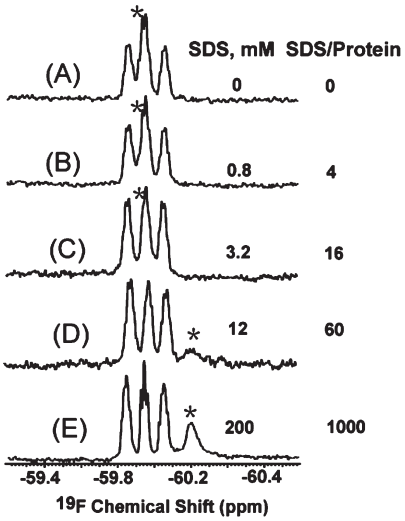

FIGURE 6: ^{19}F NMR spectra of 200 μM α-synuclein in SDS. Asterisks indicate the positions of the fY39 resonance from the free and bound forms.

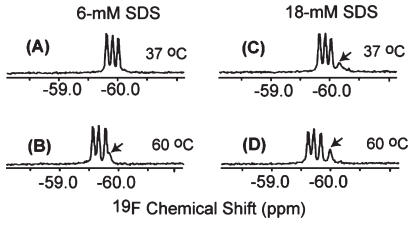

FIGURE 7: ^{19}F NMR spectra of 200 μM α-synuclein in SDS at 37 and 60 °C. An arrow indicates the position of the fY39 resonance from the bound form.

DISCUSSION

The high sensitivity and simple spectra provided by ^{19}F make this isotope an attractive probe of a complicated fibrillation process in which the protein may experience one or more conformational transitions (Figure 1B). We expressed fY-labeled α-synuclein in *E. coli* by using the method of Khan et al. (*24*). The mass data (Figure 2) show that 95% of the protein molecules contain at least one fY. The pattern of the peak heights is consistent with random fY incorporation. This conclusion is supported by the observation of nearly equal areas under each ^{19}F resonance in the NMR spectrum of the labeled wild-type protein (Figure 3). In summary, the protein synthesis system does not distinguish between tyrosine and fY, but an intracellular pool of tyrosine remains.

^{19}F as a Probe of Protein Order, Solvent Exposure, and Conformational Change. The spectra used to assign the fY resonances (Figure 3) show only a small range of ^{19}F chemical shifts (~0.3 ppm) compared to what is observed for globular proteins [up to 10 ppm (*20*, *24*)]. This limited dispersion is consistent with the known disorder of α-synuclein. Nevertheless, each fY resonance is resolved.

The solvent exposure of the labeled side chains can be assessed with ^{19}F NMR by examining the change in chemical shift on replacing H_2O with D_2O. When the fluorine atom is completely solvent exposed, its chemical shift can change by up to 0.25 ppm (*26*). Solvent isotope effects are observed for all of the labeled tyrosines in α-synuclein (Figure 4), consistent with the idea that the protein has only transient structure.

^{19}F NMR can provide insight into transient structure through the examination of cosolute-induced shifts. We examined spectra of α-synuclein in buffer, 8 M urea, and 200 mM SDS (Figure 5). The cosolute urea destabilizes secondary structure. Adding urea (Figure 5B) causes minimal changes in the chemical shifts of the three C-terminal tyrosines, but a larger change is observed for the resonance from fY39. This observation indicates that although the C-terminal region is disordered, the N-terminal region possesses some residual structure that is lost upon adding urea. This conclusion is consistent with data showing that α-synuclein

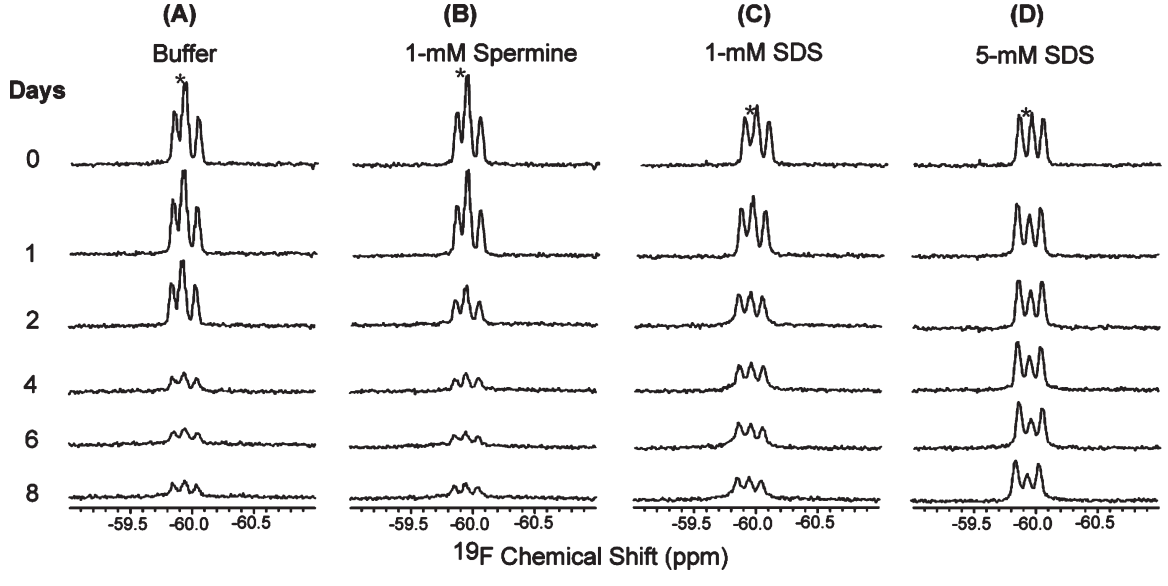

FIGURE 8: ^{19}F NMR spectra of 200 μM α-synuclein in buffer (A), 1 mM spermine (B), 1 mM SDS (C), and 5 mM SDS (D) as a function of time. An asterisk indicates the position of the fY39 resonance from the free form.

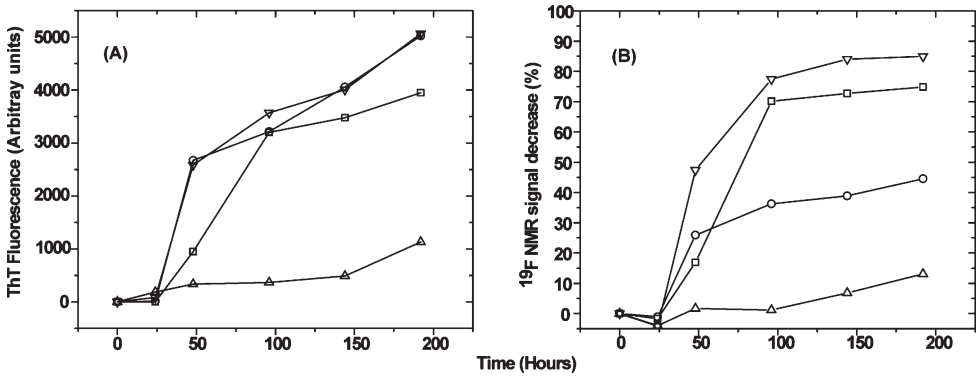

FIGURE 9: Fibrillation of α-synuclein monitored by ThT fluorescence (A) and ^{19}F NMR (B) (□, buffer; ○, 1 mM SDS; △, 5 mM SDS; ▽, 1 mM-spermine). The lines connecting the points are of no theoretical significance.

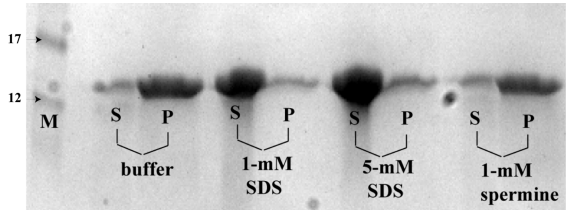

FIGURE 10: SDS−PAGs of α-synuclein fibrillation products. Conditions are given on the figure (S, supernatant; P, pellet). Lane 1 is a marker with molecular masses indicated in kDa.

adopts a compact conformation and has residual N-terminal α-helical structure in buffer (*27*−*31*).

α-Synuclein is mainly helical in SDS solution (*32*−*34*). The critical micelle concentration of SDS under the conditions used here is less than 0.1 mM, and each micelle comprises about ∼100 SDS molecules (*4*, *35*). Adding SDS to a concentration of 5 mM causes the fY39 resonance to both shift and broaden (Figure 5C), but the resonances from other residues are less affected. We conclude that the side chain of fY39 interacts with the SDS micelle, constraining its nanosecond motion. We also conclude that SDS does not induce helix formation in the C-terminal region of the protein. These conclusions demonstrate that ^{19}F NMR is a good probe of conformational change at the resolution of individual residues.

^{19}F NMR as a Probe of SDS-Bound α-Synuclein. ^{15}N NMR data show that α-synuclein changes from a collapsed ensemble in buffer to an ensemble comprising two curved, antiparallel helices with a mobile C-terminus in solutions of SDS micelles (*34*, *36*). The ^{15}N resonances from the central region of the protein broaden beyond detection at a molar ratio of SDS to α-synuclein of 30 or less (*34*). These resonances reappear at higher ratios, and their chemical shifts stop changing at a ratio of ∼100 (*34*, *36*).

The ^{19}F data allow us to focus separately on the environment near position fY39 and the environment of the other three tyrosines near the C-terminus of the protein. As shown in Figure 6, the resonances of the C-terminal region do not change with SDS concentration. This independence shows that the C-terminal end of the protein remains unstructured at all SDS concentrations studied.

The fY39 resonance tells a more nuanced story. Its intensity decreases from 0 M SDS to an SDS-to-α-synuclein molar ratio of 16:1. By a ratio of 60:1, the fY39 resonance has disappeared, and a new, broad, fY39 resonance begins to appear at −60.2 ppm. We interpret this disappearance and reappearance as evidence of the binding of α-synuclein to SDS micelles. The change in chemical shift indicates a change in structure around fY39 upon binding micelles. The chemical shift of the new fY39 resonance does not change on adding more SDS, indicating that the −60 ppm resonance reflects the environment of the fully formed and micelle-bound form. Although the shift does not change, the intensity of the new resonance increases with SDS concentration. This increase indicates an increase in the population of the SDS−micelle-bound form.

The disappearance of the free fY39 resonance and the broad nature of the new fY39 resonance in 12 mM SDS are consistent with the results of the ^{15}N study, but the ^{19}F NMR data provide additional information. Assuming that the breadth is caused by exchange between the micelle-bound form and free forms, the observation of resonances from both forms allows us to estimate that their exchange rate is about the same as the difference in their resonance frequencies ($\sim 10^2$ s^{-1}).

We tested the assumption that the breadth of the fY39 resonance in 12 mM SDS reflects exchange by adding heat. Increasing the temperature should increase the exchange rate, sharpening the resonance. This predicted sharpening is observed (Figure 7). In 6 mM SDS at 37 °C, the resonance is too broad to detect. When the temperature is increased to 60 °C, a new signal appears at −59.8 ppm. (The whole spectrum shifts because ^{19}F chemical shifts are exquisitely temperature sensitive.) In 18 mM SDS, the fY39 resonance from the micelle-bound state is visible at both 37 and 60 °C. Taken together, these data indicate that the C-terminal tyrosines do not interact with the micelles, but the side chain of tyrosine 39 does, and that exchange between the bound and free states of the protein occurs on the 10 ms time scale at protein concentrations of 200 μM in 12 mM SDS.

^{19}F NMR as a Probe of Fibrillation. The experiments described up to this point were conducted over the period of a few hours. In the following sections we focus on longer times to test the ability of ^{19}F NMR to provide information about fibrillation.

α-Synuclein most likely gains structure on forming its aggregation nucleus. Once formed, monomers are added to the nucleus to form fibrils. If there is a significant population of an intermediate, we might expect to observe new ^{19}F resonances. Solution NMR allows us to focus on the soluble monomer and small aggregates, because once fibrils form their resonances broaden beyond detection. NMR also facilitates quantification because the area under a resonance is directly related to the concentration of the species it represents.

The result for fibrillation in buffer shows what is expected (Figure 8A). That is, the resonances disappear with time as the

monomer and small aggregates form large fibrils. ^{19}F NMR data also provide information about intermediates. For instance, the observation that the chemical shifts are time-independent leads us to conclude that low molecular weight intermediates either are absent or cannot be detected.

Studies using ThT to monitor fibrillation show that low concentrations of SDS or spermine accelerate fibrillation (*4*, *37*, *38*). The NMR results for 1 mM spermine (Figure 8B) and 1 mM SDS (Figure 8C) are consistent with these observations. The acceleration is not caused by significant quantities of an NMR-detecable intermediate, because there are no chemical shift changes.

Five millimolar SDS slows fibrillation (Figure 8D). Our data on the interactions between α-synuclein and SDS (Figure 6), combined with properties of SDS micelles, suggest an explanation for the concentration-dependent effect of SDS on aggregation rate. As stated above, the critical micelle concentration under the conditions used here is less than 0.1 mM SDS, and there are ~100 SDS molecules per micelle (*4*, *35*). At 1 mM SDS and 200 μM α-synuclein, the average micelle has 20 molecules of bound α-synuclein. At 5 mM SDS, the average micelle has only four molecules of bound α-synuclein (*33*−*35*, *39*). In agreement with Rivers et al. (*38*), we conclude that the micelle-bound species of α-synuclein is in a more aggregation prone conformation compared to the species present in buffer alone. The presence of multiple copies of the aggregation prone molecule on the surface of a micelle accelerates aggregation. Increasing the SDS concentration dilutes the concentration of the conformation, which decreases the aggregation rate.

Comparing ThT and ^{19}F NMR as Probes of Fibrillation. The time dependence of α-synuclein fibrillation as assessed by ThT fluorescence and the area under the ^{19}F resonances is shown in Figure 9. All of the curves are consistent with the nucleation-dependent polymerization model, which comprises a nucleation phase, an exponential fibril growth (elongation) phase, and a final equilibrium phase.

ThT fluorescence is enhanced upon fibril binding. The resulting fluorescence intensity, however, is not directly related to the amount of fibril gained or the amount of monomer lost because the response of ThT depends on pH, dielectric constant, and fibril morphology (*15*, *16*, *40*). The area under the ^{19}F resonances, on the other hand, provides a direct accounting of the monomer plus small aggregates.

This advantage of NMR is illustrated by the data for fibrillation in 1 mM SDS (Figure 9). Although ThT and ^{19}F NMR data give similar kinetics (lag time phase, growth, and plateau), the ThT data do not provide reliable concentrations. Specifically, in 1 mM SDS, ThT fluorescence intensity is as high as that observed in buffer or in buffer plus spermine, but the NMR data show that only ~45% α-synuclein forms fibrils in 1 mM SDS, compared to 75−85% in buffer and spermine. These results are confirmed by SDS−PAG electrophoresis (Figure 10). Taken together, our data show that although 1 mM SDS and 1 mM spermine accelerate aggregation compared to buffer alone, the species formed in SDS are smaller than those formed in buffer or buffer plus spermine. To the best of our knowledge, these results are the first quantitative analysis of protein fibrillation using ^{19}F NMR.

ACKNOWLEDGMENT

We thank Carol Parker for performing the mass spectrometry experiments, Marc ter Horst for maintaining the NMR spectrometer, David Lawrence for the use of the fluorometer, the Pielak group for insightful discussions, and Elizabeth Pielak for comments on the manuscript.

REFERENCES

1. Uversky, V. N. (2007) Neuropathology, biochemistry, and biophysics of α-synuclein aggregation. *J. Neurochem. 103*, 17–37.
2. Fernandez, C. O., Hoyer, W., Zweckstetter, M., Jares-Erijman, E. A., Subramaniam, V., Griesinger, C., and Jovin, T. M. (2004) NMR of α-synuclein-polyamine complexes elucidates the mechanism and kinetics of induced aggregation. *EMBO J. 23*, 2039–2046.
3. Fink, A. L. (2006) The aggregation and fibrillation of α-synuclein. *Acc. Chem. Res. 39*, 628–634.
4. Necula, M., Chirita, C. N., and Kuret, J. (2003) Rapid anionic micelle-mediated α-synuclein fibrillization in vitro. *J. Biol. Chem. 278*, 46674–46680.
5. Munishkina, L. A., Cooper, E. M., Uversky, V. N., and Fink, A. L. (2004) The effect of macromolecular crowding on protein aggregation and amyloid fibril formation. *J. Mol. Recognit. 17*, 456–464.
6. Uversky, V. N., Li, J., and Fink, A. L. (2001) Evidence for a partially folded intermediate in alpha-synuclein fibril formation. *J. Biol. Chem. 276*, 10737–10744.
7. Dedmon, M. M., Lindorff-Larsen, K., Christodoulou, J., Vendruscolo, M., and Dobson, C. M. (2005) Mapping long-range interactions in α-synuclein using spin-label NMR and ensemble molecular dynamics simulations. *J. Am. Chem. Soc. 127*, 476–477.
8. Sandal, M., Valle, F., Tessari, I., Mammi, S., Bergantino, E., Musiani, F., Brucale, M., Bubacco, L., and Samori, B. (2008) Conformational equilibria in monomeric α-synuclein at the single-molecule level. *PLoS Biol. 6*, e6.
9. Wu, K. P., Kim, S., Fela, D. A., and Baum, J. (2008) Characterization of conformational and dynamic properties of natively unfolded human and mouse α-synuclein ensembles by NMR: implication for aggregation. *J. Mol. Biol. 378*, 1104–1115.
10. Spillantini, M. G., Schmidt, M. L., Lee, V. M., Trojanowski, J. Q., Jakes, R., and Goedert, M. (1997) α-Synuclein in Lewy bodies. *Nature 388*, 839–840.
11. Heise, H., Hoyer, W., Becker, S., Andronesi, O. C., Riedel, D., and Baldus, M. (2005) Molecular-level secondary structure, polymorphism, and dynamics of full-length α-synuclein fibrils studied by solid-state NMR. *Proc. Natl. Acad. Sci. U.S.A. 102*, 15871–15876.
12. Vilar, M., Chou, H. T., Luhrs, T., Maji, S. K., Riek-Loher, D., Verel, R., Manning, G., Stahlberg, H., and Riek, R. (2008) The fold of α-synuclein fibrils. *Proc. Natl. Acad. Sci. U.S.A. 105*, 8637–8642.
13. Wood, S. J., Wypych, J., Steavenson, S., Louis, J. C., Citron, M., and Biere, A. L. (1999) α-Synuclein fibrillogenesis is nucleation-dependent. Implications for the pathogenesis of Parkinson's disease. *J. Biol. Chem. 274*, 19509–19512.
14. LeVine, H.III (1999) Quantification of β-sheet amyloid fibril structures with thioflavin T. *Methods Enzymol. 309*, 274–284.
15. Khurana, R., Coleman, C., Ionescu-Zanetti, C., Carter, S. A., Krishna, V., Grover, R. K., Roy, R., and Singh, S. (2005) Mechanism of thioflavin T binding to amyloid fibrils. *J. Struct. Biol. 151*, 229–238.
16. Krebs, M. R., Bromley, E. H., and Donald, A. M. (2005) The binding of thioflavin-T to amyloid fibrils: localisation and implications. *J. Struct. Biol. 149*, 30–37.
17. Pedersen, J. S., Dikov, D., Flink, J. L., Hjuler, H. A., Christiansen, G., and Otzen, D. E. (2006) The changing face of glucagon fibrillation: structural polymorphism and conformational imprinting. *J. Mol. Biol. 355*, 501–523.
18. Kaylor, J., Bodner, N., Edridge, S., Yamin, G., Hong, D. P., and Fink, A. L. (2005) Characterization of oligomeric intermediates in α-synuclein fibrillation: FRET studies of Y125W/Y133F/Y136F α-synuclein. *J. Mol. Biol. 353*, 357–372.
19. Dusa, A., Kaylor, J., Edridge, S., Bodner, N., Hong, D. P., and Fink, A. L. (2006) Characterization of oligomers during α-synuclein aggregation using intrinsic tryptophan fluorescence. *Biochemistry 45*, 2752–2760.
20. Danielson, M. A., and Falke, J. J. (1996) Use of ^{19}F NMR to probe protein structure and conformational changes. *Annu. Rev. Biophys. Biomol. Struct. 25*, 163–195.
21. Eccleston, J. F., Molloy, D. P., Hinds, M. G., King, R. W., and Feeney, J. (1993) Conformational differences between complexes of elongation factor Tu studied by ^{19}F-NMR spectroscopy. *Eur. J. Biochem. 218*, 1041–1047.
22. Frieden, C., Hoeltzli, S. D., and Ropson, I. J. (1993) NMR and protein folding: equilibrium and stopped-flow studies. *Protein Sci. 2*, 2007–2014.

23. Winkler, G. R., Harkins, S. B., Lee, J. C., and Gray, H. B. (2006) α-Synuclein structures probed by 5-fluorotryptophan fluorescence and ^{19}F NMR spectroscopy. *J. Phys. Chem. 110*, 7058–7061.
24. Khan, F., Kuprov, I., Craggs, T. D., Hore, P. J., and Jackson, S. E. (2006) ^{19}F NMR studies of the native and denatured states of green fluorescent protein. *J. Am. Chem. Soc. 128*, 10729–10737.
25. Conway, K. A., Lee, S. J., Rochet, J. C., Ding, T. T., Williamson, R. E., and Lansbury, P. T., (2000) Acceleration of oligomerization, not fibrillization, is a shared property of both α-synuclein mutations linked to early-onset Parkinson's disease: implications for pathogenesis and therapy. *Proc. Natl. Acad. Sci. U.S.A. 97*, 571–576.
26. Hull, W. E., and Sykes, B. D. (1976) Fluorine-19 nuclear magnetic resonance study of fluorotyrosine alkaline phosphatase: the influence of zinc on protein structure and a conformational change induced by phosphate binding. *Biochemistry 15*, 1535–1546.
27. Eliezer, D., Kutluay, E., Bussell, R. Jr., and Browne, G. (2001) Conformational properties of α-synuclein in its free and lipid-associated states. *J. Mol. Biol. 307*, 1061–1073.
28. Kim, H.-Y., Heise, H., Fernandez, C. O., Baldus, M., and Zweckstetter, M. (2007) Correlation of amyloid fibril β-structure with the unfolded state of α-synuclein. *ChemBioChem 8*, 1671–1674.
29. Sung, Y.-h., and Eliezer, D. (2007) Residual structure, backbone dynamics, and interactions within the synuclein family. *J. Mol. Biol. 372*, 689–707.
30. Morar, A. S., Olteanu, A., Young, G. B., and Pielak, G. J. (2001) Solvent-induced collapse of α-synuclein and acid denatured cytochrome *c*. *Protein Sci. 10*, 2195–2199.
31. Bertoncini, C. W., Jung, Y. S., Fernandez, C. O., Hoyer, W., Griesinger, C., Jovin, T. M., and Zweckstetter, M. (2005) Release of long-range tertiary interactions potentiates aggregation of natively unstructured alpha-synuclein. *Proc. Natl. Acad. Sci. U.S.A. 102*, 1430–1435.
32. Ferreon, A. C. M., Gambin, Y., Lemke, E. A., and Deniz, A. A. (2009) Interplay of α-synuclein binding and conformational switching probed by single-molecule fluorescence. *Proc. Natl. Acad. Sci. U.S.A. 106*, 5645–5650.
33. Veldhuis, G., Segers-Nolten, I., Ferlemann, E., and Subramaniam, V. (2009) Single-molecule FRET reveals structural heterogeneity of SDS-bound α-synuclein. *ChemBioChem 10*, 436–439.
34. Ulmer, T. S., Bax, A., Cole, N. B., and Nussbaum, R. L. (2005) Structure and dynamics of micelle-bound human α-synuclein. *J. Biol. Chem. 280*, 9595–9603.
35. Croonen, Y., Gelade, E., Van der Zegel, M., Van der Auweraer, M., Vandendriessche, H., De Schryver, F. C., and Almgren, M. (1983) Influence of salt, detergent concentration, and temperature on the fluorescence quenching of 1-methylpyrene in sodium dodecyl sulfate with m-dicyanobenzene. *J. Phys. Chem. B 87*, 1426–1431.
36. Bisaglia, M., Tessari, I., Pinato, L., Bellanda, M., Giraudo, S., Fasano, M., Bergantino, E., Bubacco, L., and Mammi, S. (2005) A topological model of the interaction between α-synuclein and sodium dodecyl sulfate micelles. *Biochemistry 44*, 329–339.
37. Antony, T., Hoyer, W., Cherny, D., Heim, G., Jovin, T. M., and Subramaniam, V. (2003) Cellular polyamines promote the aggregation of α-synuclein. *J. Biol. Chem. 278*, 3235–3240.
38. Rivers, R. C., Kumita, J. R., Tartaglia, G. G., Dedmon, M. M., Pawar, A., Vendruscolo, M., Dobson, C. M., and Christodoulou, J. (2008) Molecular determinants of the aggregation behavior of α- and β-synuclein. *Protein Sci. 17*, 887–898.
39. Newbery, J. E. (1979) The variation of the critical micelle concentration of sodium dodecyl sulphate with ionic strength monitored by selective-ion membrane electrodes. *Colloid Polym. Sci. 257*, 773–775.
40. Maskevich, A. A., Stsiapura, V. I., Kuzmitsky, V. A., Kuznetsova, I. M., Povarova, O. I., Uversky, V. N., and Turoverov, K. K. (2007) Spectral properties of thioflavin T in solvents with different dielectric properties and in a fibril-incorporated form. *J. Proteome Res. 6*, 1392–1401.